DOI: 10.61782/fa.2025.0623

FORUM ACUSTICUM EURONOISE 2025

NON-INVASIVE AND LOW-COST PHOTOACOUSTIC/ULTRASOUND DUAL-MODAL IMAGING SYSTEM FOR CAROTID PLAQUE IMAGING

Alejandro Ariza-Carrasco[1,2] **Javier G. Muñoz**[1,2] **Jorge Cruza**[3]
Luis Elvira[3] **Joaquín L. Herraíz**[1,2] **José M. Udías**[1,2]
María Alonso de Laciñana[4] **Jorge Rodríguez-Pardo**[4] **Paula Ibáñez García**[1,2]
Mailyn Pérez-Liva[1,2*]

[1] Department of Matter Structure, Thermal and Electronic Physics and IPARCOS, Complutense University of Madrid, Madrid, Spain
[2] Departamento de Estructura de la Materia, Física Térmica y Electrónica, Facultad de Ciencias Físicas, Universidad Complutense de Madrid (UCM); IdISSC, España.
[3] Ultrasound Systems and Technology Group (GSTU), Institute for Physical and Information, Spanish National Research Council (CSIC), Madrid, Spain
[4] Department of Neurology and Stroke Centre, Neurological Sciences and Cerebrovascular Research Laboratory, Neurology and Cerebrovascular Disease Group, Neuroscience Area Hospital La Paz Institute for Health Research, IdiPAZ (La Paz University Hospital, Universidad Autónoma de Madrid), Madrid, Spain

ABSTRACT

Carotid plaque rupture causes most ischemic strokes, yet current diagnostics focus on arterial stenosis, overlooking 80–90% of vulnerable plaques. This highlights the need for affordable, precise, and non-invasive imaging to assess plaque vulnerability. To address this, we developed a low-cost, dual Ultrasound/Photoacoustic system integrating a Vermon L7.5-MHz ultrasound probe, a 128-channel programmable phased array Ultrasound scanner (Dasel, Spain), and pannels of pulsed semiconductor lasers diodes of 5W emitting 100 ns pulses at 447 nm. Synchronization was managed via external pulse generators, with laser light delivered through optical fibers. Validation utilised phantoms of black nylon threads. GPU-accelerated delay-and-sum beamforming was used for image recontruction. The system achieved 530 μm lateral and 360 μm axial resolution. This system offers a cost-effective, non-invasive approach for high-resolution multiparametric tissue characterization. Future aims will be to improve in vivo assessment of plaque vulnerability.

Keywords: *photoacoustic, delay-and-sum, lateral and axial resolution, signal-to-noise ratio, low-cost*

**Corresponding author*: *mailyn01@ucm.es.*

1. INTRODUCTION

Stroke causes over 11.6% of all deaths, with ischaemic stroke alone responsible for more than 6 million deaths annually, making it the second leading cause of death worldwide. It is primarily triggered by plaques in the carotid artery—mainly composed of lipids, blood, and collagen—that obstruct blood flow and rupture suddenly. While our understanding of plaque evolution has advanced, current diagnostics still focus mainly on detecting arterial stenosis. This approach only identifies 10-20% of cases, thereby missing crucial indicators of plaque vulnerability [1]. Consequently, there is an urgent need for non-invasive, simple, and low-cost imaging techniques that can assess carotid plaques' composition, stability and vulnerability.

Photoacoustic imaging (PAI) is a promising technique that combines the contrast and spectral benefits of optical imaging with the deep penetration and high spatial resolution of ultrasound, taking advantage of the low scattering of ultrasound in biological tissue and relying on the photoacoustic (PA) effect [2]. This effect is produced by illuminating the tissue with pulsed light of very short duration (around a few nanoseconds), which causes the molecules present, whether endogenous or exogenous (such as haemoglobin or melanin), to absorb the incident energy. This absorption generates a local increase in temperature and pressure, which in turn causes a thermoelastic expansion of the tissue, giving rise to acoustic waves that propagate and are picked up by ultrasound transducers. In this way, the technique complements ultrasound information by providing functional data on tissue oxygenation and vascular dynamics. The study aims to characterize a low-cost, portable ultrasound-photoacoustic system using semiconductor laser diodes, which are more affordable and portable than traditional lasers.

2. METHODOLOGY

2.1 System description

We developed a low-cost, non-invasive dual Ultrasound/Photoacoustic system. This system consists of a clinical ultrasound probe (Vermon L7.5 MHz) with 128 elements, a centre frequency of 7.5 MHz and a bandwidth of 60%. For the photoacoustic part, the system consists of two panels of five pulsed semiconductor laser diodes (SLD) with a wavelength of 447 nm and 5W of power, placed on each side of the clinical probe. The illumination from each diode is delivered uniformly to the transducer's acquisition plane via optical fibers attached to each diode on the panels (Fig. 1). The delivered pulse width is 100 ns with a pulse repetition rate of 1 kHz. This pulse generated by the diodes is regulated by an Arduino signal generator (Arduino Uno) and a controller (SLD Picolas LDP-V 240-100 V3.3 Driver) that is responsible for activating and synchronising the illumination and ultrasound detection. The images are acquired by a programmable ultrasound scanner provided by the company Dasel (Spain), with a sampling frequency of 62.5 MHz and 128 transmission and reception channels. This scanner can perform multiple acquisitions, allowing the use of different types of averaging to minimise the noise characteristic of photoacoustic images. The acquired photoacoustic images have a depth of 20 mm, since this depth marks the practical limit of imaging in the current photoacoustic configuration, since from that point the intensity of the fluence is 20% lower than its maximum value.

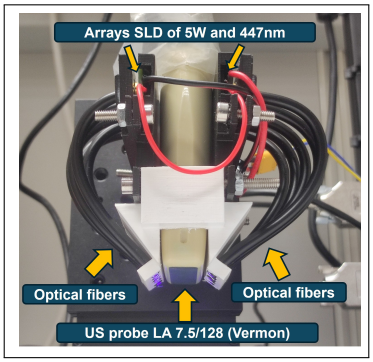

Figure 1. Photoacoustic system that combines a clinical ultrasound probe with two arrays of five 5W SLD (447 nm). These diodes are attached to the sides of the probe, and their light is delivered to the transducer's acquisition plane through optical fibers.

2.2 Image reconstruction

After the photoacoustic signal is captured by the ultrasound detectors, reconstruction algorithms are employed to convert the temporal variations in pressure into final photoacoustic images. Numerous reconstruction methods are now available to achieve this, and the GPU-accelerated delay and summation (DAS) method was used in this study [3].

2.3 Lateral and axial resolution

To evaluate spatial resolution, a home-made phantom of 0.26 mm diameter black nylon threads spaced 4 mm apart both laterally and axially (Fig 3A.), immersed in water, was scanned with our experimental setup. The following expressions were used to calculate the theoretical and lateral resolution [4]:

$$R_l = 0.71 \cdot \frac{c_0}{NA \cdot f_0} \qquad R_a = 0.88 \cdot \frac{c_0}{\Delta f} \tag{1}$$

with c_0 the velocity of sound in the medium, NA is the numerical acoustic aperture, f_0 and Δf the centre frequency and bandwidth of the transducer signal, respectively. To characterise the spatial resolution of our system we reconstructed the image of a point target, in this case

the black nylon thread, and used the Point Spread Function (PSF) method [4]. The Full Width at Half Maximum (FWHM) of the PSF determines our experimental spatial resolution.

2.4 Signal-to-noise ratio (SNR) and amplitude correction map

Several photoacoustic image acquisitions were performed to test the dependence of signal-to-noise ratio (SNR) on the number of averaged signals. Finally, an amplitude correction of the reconstructed PA image with DAS of the black nylon phantom was performed. For this purpose, the reconstructed image was divided into blocks and, for each block, the maximum amplitude value is extracted. This generates a 'correction map' representing the local variation of the signal in the image. This map is used to normalise the original image by dividing the reconstructed image by the correction map, thus compensating for acoustic and optical attenuations and local variations in amplitude, resulting in a more homogeneous representation of the signal. Finally, a median filter was applied, reducing residual noise and improving the visual quality of the corrected image.

3. RESULTS

3.1 Lateral and axial resolution evaluation

The theoretical lateral and axial resolution of the system were obtained to be 0.23 mm and 0.29 mm, respectively. However, these theoretical resolutions are not taking into account in their expressions the characteristics of the piezoelectric elements of the transducer such as kerf or pitch. On the other hand, Fig. 2B shows the photoacoustic image reconstructed with the delay-and-sum algorithm of the black nylon thread (Fig. 2A) immersed in water. From the PSF method, we extracted the FWHM of the reconstructed signal, previously performing a Gaussian fit to it and establishing that if the signal did not exceed a threshold of -6 dB then the system is not able to correctly resolve the point object. By analysing both the lateral and axial profiles of the signal, we obtained a lateral resolution of $R_L = 0.53$ mm and an axial resolution of $R_A = 0.36$ mm (Fig. 2C).

3.2 SNR vs number of signal averages and correction amplitude of the reconstructed images

To determine the optimal number of image averages for our acquisitions, we analyzed the SNR as a function of

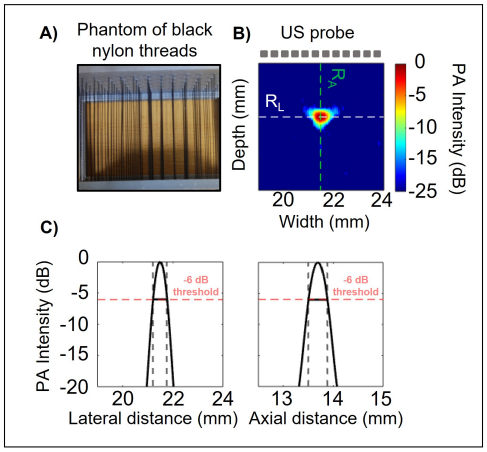

Figure 2. A) A phantom with 0.26 mm diameter black nylon threads spaced 4 mm apart laterally and axially. B) A PA image of the threads is reconstructed using DAS to assess the lateral and axial signal profiles. C) The lateral and axial resolutions are determined via the PSF method, using a -6 dB threshold as the resolvability limit.

the number of averaged frames. As shown in Fig. 3, the SNR progressively improves with the number of acquisitions. A noticeable increase is observed around 3000 averages, where the SNR reaches approximately 54%, indicating a significant enhancement in signal clarity. At 5000 and 10000 averages, the SNR further improves by roughly 30%. Based on these results, we selected 5000 averages as a suitable trade-off, providing a robust SNR of 72% while keeping the acquisition time within 5 seconds, making the system more suitable for time-sensitive applications.

Finally, a photoacoustic image of the phantom composed of black nylon threads was reconstructed using the DAS algorithm (Fig. 4A). An amplitude correction was subsequently applied to account for signal attenuation with depth and laterally (Fig. 4B). As illustrated in Fig. 4C, the corresponding amplitude profiles show a marked improvement, exhibiting a more homogeneous signal distribution across all the image. This indicates that the amplitude correction effectively compensates for intensity decay, enhancing the overall image uniformity and interpretability.

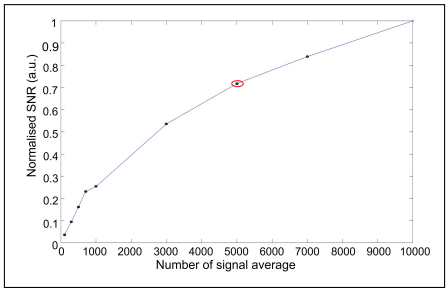

Figure 3. Normalised Signal-to-noise ratio (SNR) as a function of the number of signal averages. The red circle indicates the averaged signal number we chose to perform the rest of the measurements, since it represents 0.72 SNR, indicating a good signal-to-noise ratio.

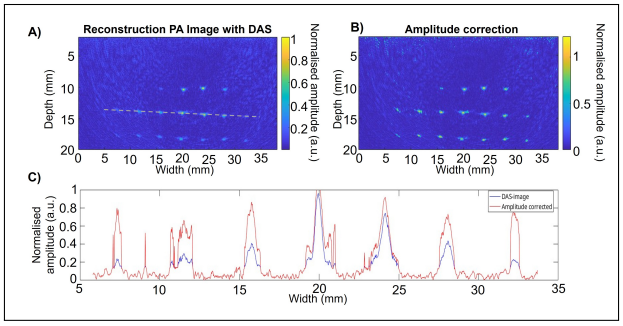

Figure 4. A) Normalized PA image of the black nylon threads phantom reconstructed with DAS. B) The image after amplitude correction. C) Amplitude profiles showing the original image in blue and the corrected image in red, with the dotted line indicating the DAS-extracted profile.

4. CONCLUSIONS AND FUTURE WORK

We developed a low-cost, non-invasive dual ultrasound/photoacoustic imaging system capable of delivering high-quality imaging performance, validated using black-wire phantom experiments. The system achieved a lateral resolution of 0.53 mm and an axial resolution of 0.36 mm, with a signal-to-noise ratio (SNR) of 0.72 obtained from 5000 averaged acquisitions. These results confirm the system's robustness and suitability for high-contrast, depth-resolved imaging.

Future work will focus on the ex vivo characterization of resected human atherosclerotic plaques under the ethical approval PI-6157 (La Paz University Hospital of Madrid, Spain). This next step aims to assess the system's ability to differentiate plaque composition and support the identification of features related to vulnerability, ultimately advancing its potential for clinical vascular imaging applications.

5. ACKNOWLEDGMENTS

This work received support from the European Union's Horizon 2020 research and Innovation Programme under the Marie Sklodowska-Curie Grant Agreement no.101030046, and the Programme Ramón y Cajal RYC2021-032739-I, funded by MCIN/AEI/10.13039/501100011033 and by the European Union "NextGenerationEU"/PRTR". Also, we acknowledge support from grants FASCINA (PID2021-126998OB-I00/), 3PET (PDC2022-133057-I00) from the Spanish Ministry of Science and Innovation (MCIN) AEI/10.13039/501100011033/Unión Europea Next GenerationEU/PRTR, Prototwin Project (TED2021-349 130592B-I00) and Tecnologías Avanzadas para la Exploración del Universo y sus Componentes" (PR47/21 TAU-CM TAU- PRTR), funded by EU Resilient and NextGeneration funds. This work was supported by Knowledge Generation Projects 2022 Type A Oriented Research, Government of Spain INVENTOR (PID2022-137114OA-I00).

6. REFERENCES

[1] G. . S. Collaborators, "Global, regional, and national burden of stroke and its risk factors, 1990–2019: a systematic analysis for the global burden of disease study 2019.," *The Lancet. Neurology*, vol. 20, no. 10, p. 795, 2021.

[2] M. Xu and L. V. Wang, "Photoacoustic imaging in biomedicine.," *Review of scientific instruments*, vol. 77, no. 4, p. 041101, 2006.

[3] V. Perrot, M. Polichetti, F. Varray, and D. Garcia, "So you think you can das? a viewpoint on delay-and-sum beamforming.," *Ultrasonics*, vol. 111, p. 106309, 2021.

[4] I. Pi-Martín, A. Cebrecos, J. J. García-Garrigós, N. Jiménez, and F. Camarena, "Spatial resolution and reconstructed size accuracy using advanced beamformers in linear array-based pat systems.," *Photoacoustics*, vol. 34, p. 100576, 2023.